International Journal of Technology 15(6) 1712-1729 (2024)
Received July 2024 / Revised August 2024 / Accepted September 2024

International Journal of Technology

http://ijtech.eng.ui.ac.id

Evaluation of Laplacian Spatial Filter Implementation in Detecting Driver Vigilance Using Linear Classifier

Dedik Romahadi[1,2*], Aberham Genetu Feleke[2], Rikko Putra Youlia[1]

[1]*Department of Mechanical Engineering, Faculty of Engineering, Mercu Buana University, East Meruya Street No. 1, Kembangan, West Jakarta (Postal Code 11650), Indonesia*
[2]*School of Mechanical Engineering, Beijing Institute of Technology, Zhongguancun South Street No. 5, Haidian District, Beijing (Postal Code 100081), China*

Abstract. Maintaining a high level of safety awareness among drivers is essential to ensure the safe operation of automated vehicles (AVs). Many factors can influence the model's performance in achieving accuracy, such as the application of spatial filters, the type of feature selection, and the classifier. Complex modeling, accuracy achievement, and learning time are also practically difficult. No study has discussed the application of the Laplacian Spatial Filter (LSF) to driver vigilance classification performance. Therefore, this study aimed to analyze driving vigilance detection using LSF and linear classification models. The study involved signal preprocessing and feature extraction in signal energy, followed by the application of Kruskal - Wallis (KW) and Minimum Redundancy - Maximum Relevance (MRMR) for feature selection. Finally, various classification models such as Linear Discriminant Analysis (LDA), Logistic Regression (LR), Naive Bayes (NB), and Support Vector Machine (SVM) were used for exploration. The results were significant, with SVM without LSF achieving the highest average accuracy of 84.26% in the intra-subject and 70.15% across the subject. Based on this study, LSF was not recommended for EEG-based driver vigilance detection.

Keywords: Electroencephalogram; Laplacian spatial filter; Linear classifier; Machine learning; Vigilance detection

1. Introduction

Driver vigilance is crucial for road safety, accident prevention, and meeting legal and ethical obligations as a driver. Sustaining attention and vigilance while driving diminishes hazards and improves the total safety of the driving environment for all individuals (Zainy *et al.,* 2023; Zuraida, Wijayanto, and Iridiastadi, 2022). The main objective of automated driving, which uses computer systems and artificial intelligence, is to significantly reduce accidents caused by human error (Gan *et al.,* 2023; Zhou, 2023). Despite the current cognitive deficiencies in most AVs (Cui *et al.,* 2022), this potential of automated driving is a promising step towards a safer driving environment. According to the benchmarks set by the Society of Automotive Engineers (SAE), most AVs are found to operate at the L3 stage.

Fundamentally, current automated driving software lacks the cognitive capacity to quickly predict and evaluate potential dangers, especially when faced with accidents or "edge cases," including uncontrolled circumstances. Ensuring a trained safety driver

*Corresponding author's email: dedik.romahadi@mercubuana.ac.id, Tel.: +62-215840815;
Fax.: +62-215871335
doi: 10.14716/ijtech.v15i6.7166

constantly supervises these AVs is crucial (Gupta *et al.,* 2023; Pranoto *et al.,* 2023). To achieve this aim, the company has recruited and provided safety training to its fleet of vehicles. Driver distraction and challenges in maintaining focus are often observed in the context of automated driving. In this scenario, securing control of an unwary driver usually takes a long time. A study showed that performing a monotonous driving task for 30 minutes could affect the ability of an individual to maintain vigilance (Li *et al.,* 2023a; Oztel, 2021). Therefore, monitoring the safety attention of the driver is very important.

Previous methods primarily rely on four distinct sources of information: physical characteristics, vehicle characteristics, physiological signals, and information from multiple sources (Luna *et al.,* 2022). Vehicle characteristics include braking distance, lane departure, speed, and steering control. When drivers feel hyper-vigilant, the ability to perform essential driving activities is reduced, affecting personal operations. (Li *et al*., 2022a; Arefnezhad *et al.,* 2019; Li *et al.,* 2017). Moreover, drivers' conduct and facial expressions can instinctively signify specific mental states (Li *et al.,* 2023B). Decreased driver attentiveness can change many physical characteristics, such as frequency of blinking, duration of eye closure, Percentage of Eye Closure (PERCLOS), stance, gaze, and nodding frequency (Li *et al.,* 2022b). As drivers become less aware, motorists tend to blink more often and keep individual eyes closed for longer, and eye movements may slow down due to reduced energy (Rogel *et al*., 2024). Using these characteristics to determine the driver's level of vigilance is an indirect method, and the detection accuracy can be improved. Additionally, physical feature-based methods are commonly susceptible to external influences such as sunglasses and low illumination at night.

Driver vigilance is closely connected through an Electroencephalogram (EEG) used to detect and analyze electrical signals from the brain. This method helps studies acquire important perceptions of brain activity (Othmani *et al.,* 2023; Nurfirdausi *et al.,* 2022; Bi Xia, and Fei 2021; Teng, Bi, and Liu, 2018). EEG is a time series signal often reliable for assessing vigilance (Zhang and Eskandarian, 2021; Zhang and Etemad, 2021). However, the raw form of the EEG signal, which represents changes in electrical potential over time, cannot be directly used to assess vigilance (Wang *et al.,* 2023; Yu *et al.,* 2019). The signal frequency band changes' power spectrum is often used to evaluate vigilance. Following this discussion, spatial filters make records more closely resemble those obtained with ideal reference electrodes by removing global noise and increasing the activity of local sources under the electrodes to improve signal extraction. The bibliography uses various spatial filtering methods to improve the features of multiple types of EEG signals. A study by Alonso and Vellasco (2016) explained that the filtering methods are evaluated to identify individuals capable of increasing brain signal characteristics and improving classification accuracy. Laplacian Spatial Filter (LSF) produced the highest average results, showing a 10% increase in proper classification compared to unfiltered data. Tsuchimoto *et al.* (2021) concluded that LSF outperformed in increasing the ratios of noise level to isolate sensorimotor behavior from EEG.

Previous studies show that using LSF has a beneficial effect on EEG categorization outcomes. However, the impact of the algorithm of LSF on driver vigilance-based EEG classification performance remains uncertain. Achieving high accuracy and reducing learning time when using complex artificial neural networks is challenging. Therefore, this study aimed to compare the classification performance of linear models with and without using LSF. The investigation uses a dataset on driving tasks totaling eight subjects conducted at night, previously published in (Zheng and Lu, 2017). The linear classification

models used include Linear Discriminant Analysis (LDA), Logistic Regression (LR), Naive Bayes (NB), and Support Vector Machine (SVM). Considering how effectively these models can handle EEG data (Nacpil *et al.,* 2023; Gaur *et al.,* 2021; Di *et al.,* 2019; Sharmila and Geethanjali, 2016), the study understands that linear classification algorithms have significant potential as the most effective way to process EEG signals. Moreover, this finding also applies feature selection using Kruskal - Wallis (KW) and Minimum Redundancy - Maximum Relevance (MRMR), which aims to optimize accuracy and learning time (Lazcano-Herrera *et al.,* 2023; Siuly *et al.,* 2020). The results of this study show the effect of applying LSF on the performance of each linear classification model.

2. Methods

2.1. Dataset

Detailed experiments were conducted on public datasets to evaluate the performance of the classification model against LSF implementation. EEG collection of driving data named SEED-VIG collected private data transferred locally, which was supplied by (Zheng and Lu, 2017). Additionally, the dataset contained EEG, EOG (Electrooculogram), and eye movement data from 23 participants using a driving task simulation system. The view of the highway was projected onto an LCD screen in front of the modified vehicle to copy real-life events, as shown in Figure 1. Following this discussion, the simulated driving settings in virtual reality consisted of various weather conditions and road types.

Figure 1 Driving simulation scenarios.

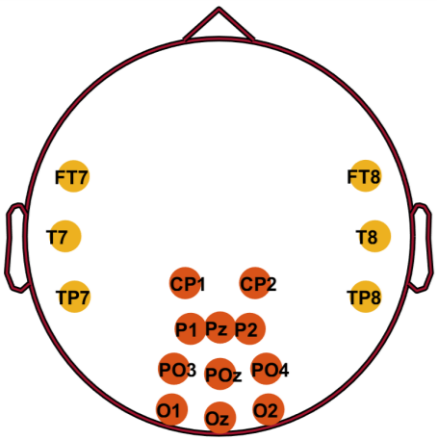

Figure 2 Placement of electrodes for EEG measurement.

The Neuroscan system and eye-tracking glasses captured forehead EOG, EEG, and simultaneous eye motions during the study. The simulated driving studies were conducted in cars without extra engines and other parts. In the experiments, the participants were instructed to operate the vehicle using the steering mechanism and accelerator foot pedal. The driving scenarios were modified in real-time based on the subject's actions. Moreover, subjects do not receive any form of feedback after sleeping.

The Neuroscan ESI measuring device acquired EEG and EOG systems with a frequency sampling of 1000 Hz. The EEG cap had 64 electrodes and was positioned using the international 10-20 standard. In addition, the EEG function only recorded 11 posterior EEG channels and six temporal EEG channels, containing 'FT7', 'FT8', 'T7', 'T8', 'TP7', 'TP8', 'CP1', 'CP2', 'P1', 'PZ,' 'P2', 'PO3', 'POZ,' 'PO4', 'O1', 'OZ', 'O2 ' as shown in Figure 2. A total of 4-channel forehead EOGs were provided in this data set for further analysis. Recordings of EEG signals were obtained from the posterior using 11-channel and 6-channel (orange color) and temporal location (blue color), correspondingly. Following the process, an infrared camera was installed on the SMI Eye Tracking Glasses 2 to capture eye gaze and multiple ocular motions, including eye blinks, saccades, and fixations. The labels in this dataset were PERCLOS levels measured by the eye tracker, as shown in Equation 1. The interval variables are derived from the summation of blink, fixation, saccade, and *CLOS*. The subject was annotated as awake when the PERCLOS level was less than 0.35. This subject was declared drowsy when the PERCLOS value was higher than 0.7. During the study, the subject was annotated tired between 0.35 and 0.7.

$$PERCLOS = \frac{blink+CLOS}{\text{interval}} \tag{1}$$

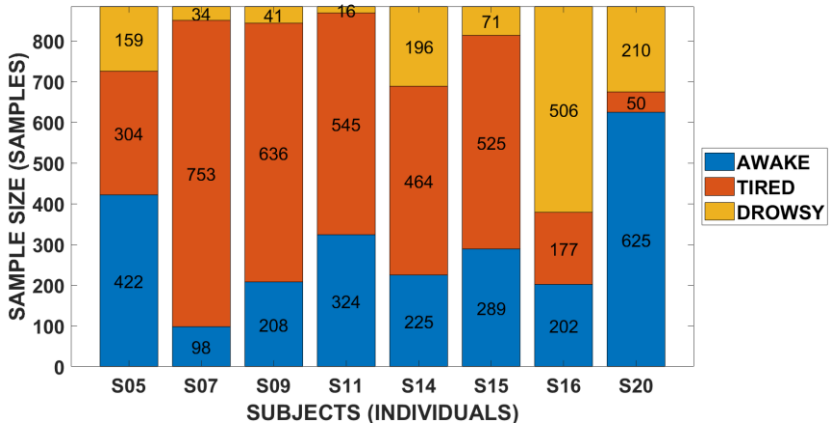

Figure 3 Number of samples for each class in each subject

The 17-channel dataset contained the same experimental tasks but allowed the generation of different features. Assessing the volume of information in each data set to evaluate the results obtained during the classification process was important. Figure 8 shows a box diagram of the number of EEG samples for the dataset. This study selected a collection of brain signals from eight subjects obtained from night experiments. The total EEG samples from each class contained 2393 awake states, 3454 tired, and 1233 drowsy samples. Moreover, one file contained EEG samples obtained from one subject. The number before each file name was used for each subject in this study. The sample size in percentage for each class is shown in Figure 3.

2.2. Tools and Materials

All computing processes were conducted on a desktop running Windows 11 64bit operating system, RTX 4080 super graphics card, on a 14th-generation Intel Core i9

processor. During the study, computing was implemented in MATLAB application version 2023b. The EOG signal in the raw EEG data was ignored, and the EEG signal was then decomposed using the Fast-ICA method (Yue *et al.,* 2022). The artifact signal was also cleaned using the Independent Component Label (IC-Label) toolbox (Pion-Tonachini, Kreutz-Delgado, and Makeig, 2019). All artifacts originating from eye blinks, heartbeats, muscle movements, and other artifacts were removed.

2.3. Preprocessing

The raw EEG data passed through processing using a band-pass finite impulse response (FIR) filter to eliminate non-brain signals. Studies have different methods for defining the boundaries of EEG frequency, but this finding selected the range of 1 - 75 Hz. The band-stop FIR filter eliminated signals with a 49 - 51 Hz frequency derived from electric current. First, the average signal was computed across all EEG electrodes and was eliminated from the EEG signal for every time point. The objective was to generate a reference that was silent or electrically neutral. Second, baseline signal correction was performed to mitigate the influence of significant aberrations in the EEG signal that exceeded acceptable limits. The EEG signal baseline was adjusted by subtracting the average time value starting at the beginning of the baseline period and continuing through the end of the stimulus phase.

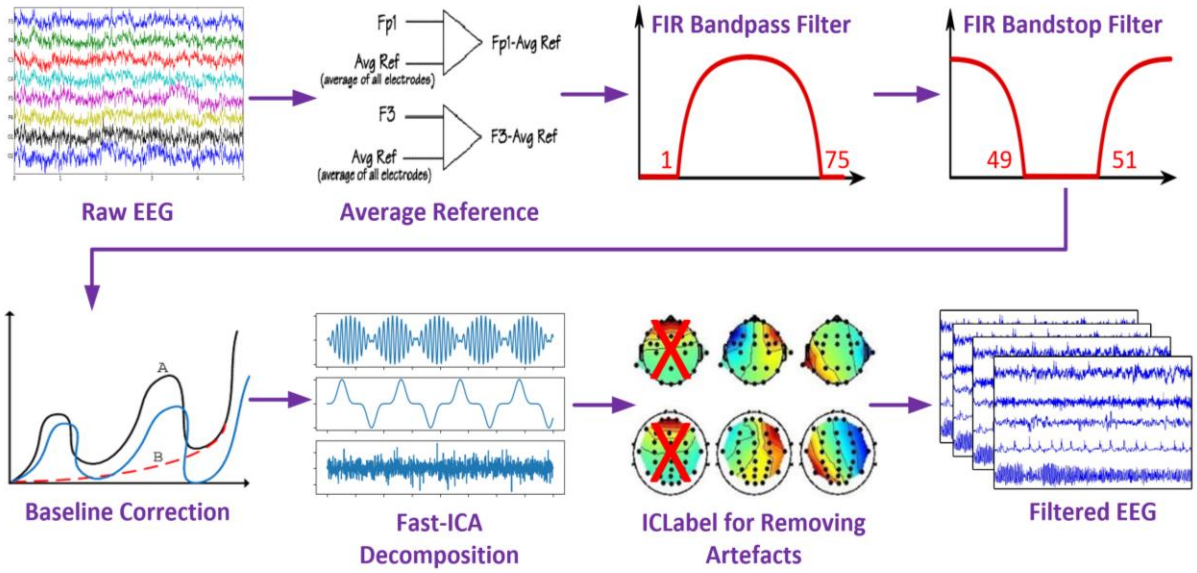

Figure 4 Pre-processing procedure of raw EEG signals

The EEG data was filtered during the study to eliminate external noise. However, internal artifacts originating from individuals, such as eye blinks, heartbeats, muscle movements, and other artifacts, had not been removed. Artifact filtering was essential for the purification of the EEG signal. Moreover, Independent Component Analysis (ICA) was implemented to characterize the constituent elements of the EEG signal. The fast-ICA algorithm used in this study (Yue *et al.,* 2022) comprised two main components, namely signal preprocessing and independent component extraction. Preprocessing consisted of two sequential steps: signal concentrating and whitening. The input data was required to be whitened for the Fast-ICA algorithm to work properly with negative entropy. Following the discussion, the primary method used by Fast-ICA was to repeatedly identify an unmixed EEG signal that optimized the non-Gaussian measure. The assessment of non-Gaussian data was quantified using entropy. Therefore, the algorithm selected negative entropy to compute the unmixed EEG signal. The IC-Label algorithm selected components that did not originate from the brain (Pion-Tonachini, Kreutz-Delgado, and Makeig, 2019). Immediately,

the EEG signal was purified against any interference and unwanted elements; the signal was divided into segments with an 8-second duration. Figure 4 shows the comprehensive preprocessing steps in the study.

2.4. Feature Extraction

There were two schemes for the feature extraction process, and the difference in these schemes was in the use of LSF, as shown in Figure 5. Following the preprocessing stage, a single-subject EEG data sample was represented as a matrix with dimensions of 17x1600x885. Value 17 corresponded to the number of channels, while 1600 reflected the signal duration, equivalent to 8 seconds. Before feature extraction, the energy contained in each EEG band was determined by analyzing the power in each channel. Equation 2, which represented LSF, was then applied to each EEG sample acquired from the preprocessing phase.

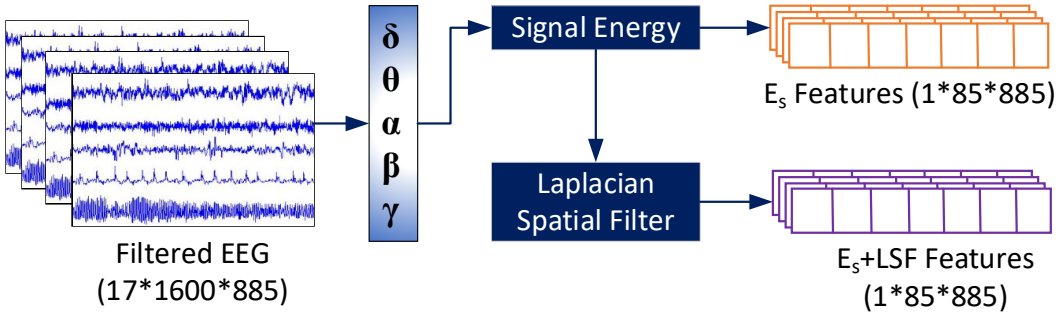

Figure 5 Procedure for extracting EEG features

$$e_i^{Laplace}(t) = e_i(t) - \frac{1}{K}\sum_j^K e_j\,(t) \tag{2}$$

LSF calculated the difference between the average value of all nearby electrodes and the value of the analyzed electrode (Alonso and Vellasco, 2016). e_i was the electrode, and j represented the index of the surrounding electrodes K. The Laplacian filtered signal was then computed according to Equation 3. Based on E_s the previously given definition, for every EEG section, E_s features were extracted from five different frequency ranges, namely delta (1–3 Hz), theta (4–7 Hz), alpha (8–12 Hz), beta (13– 30 Hz), and gamma (31–75 Hz).

$$E_s = \frac{\sum_{j=1}^{n} e_{ij}^2}{\sum_{i=1}^{m}\sum_{j=1}^{n} e_{ij}^2} \tag{3}$$

All E_s features used band-pass FIR filtering with non-overlapping 8-second signal segments. The E_s feature was obtained from the sum of voltage in each electrode squared and divided by the total sum of all electrodes squared. Since the number of samples between classes varied, the samples were multiplied using the synthetic minority oversampling techniques (SMOTE) algorithm, as shown in Equation 4. Where x was the original sample, r represented a random number between 0 and 1, j was between 1 and the nearest sample number, and z was the closest sample (Song *et al.*, 2024).

$$x_i^{'} = x_i + r \times \left(z_{ij} - x_i\right) \tag{4}$$

2.5. Feature Selection

KW (Maimaiti *et al.*, 2020; Siuly *et al.*, 2020) and MRMR (Lazcano-Herrera *et al.*, 2023) were applied to select a subset of pertinent characteristics while keeping the initial feature space intact. This process was conducted to identify the most informative features for modeling. The KW test was a non-parametric statistical test used to assess when there were

significant disparities among three or more unrelated groups of samples. The non-parametric alternative to one-way Analysis of Variance (ANOVA) was used when the usual assumptions of ANOVA, such as normality and homogeneity of variances, were not met. Following this process, the KW test statistic H was computed using Equation 5. N represented the total observation count across all groups, k was the number of clusters, Ri represented the cumulative sum of ranks for the i-th group, and ni was the aggregate quantity of observations in the i-th group.

$$H = \left(\frac{12}{N(N+1)}\right)\sum_{i=1}^{k}\frac{R_i^2}{n_i} - 3(N+1) \quad (5)$$

MRMR was a method for selecting traits that were highly related to the target variable and showed minimal overlap with one another. The objective was to improve the efficiency and clarity of the model by reducing the quantity of input features to those providing the most valuable information. Additionally, the scoring function in MRMR was generally formulated as a composite of relevance and redundancy measurements as shown in Equation 6.

$$MRMR(f_i) = Relevance(f_i, Y) - \frac{1}{|S|}\sum_{f_i \in S} Redundancy(f_i, f_j) \quad (6)$$

Where f_i was the candidate feature, and Y represented the target variable. The measurement of relevance was frequently assessed using mutual information $I(f_i; Y)$. Moreover, mutual information $I(f_i; f_j)$ was often used to measure redundancy.

2.6. Classification

After performing a significance analysis using KW and MRMR, selected feature sets were acquired. The study performed experiments using four distinct linear classification models to assess the efficacy of various characteristics in detecting driver vigilance, including LDA (Di et al., 2019), LR (Gaur *et al.,* 2021), NB (Sharmila and Geethanjali, 2016), and SVM (Nacpil *et al.,* 2023). These models were trained to use features extracted from different frequency bands applied as input. In addition, training sessions were conducted for each classifier with and without the deployment of LSF to guarantee the accuracy and dependability of the outcomes. These results were derived by calculating the average testing accuracy for each model using two classification schemes. A classification mechanism was initially implemented in each subject. This categorization method used data from the same subject for training and testing.

The second method included combining and randomizing EEG samples from eight subjects when separating the data into training and testing sets. For cross-subject classification, the study used features that produced the maximum accuracy as determined by feature selection outcomes. Training and test data sets were generated using a 5-fold cross-validation methodology.

$$Accuracy = \frac{TPs+TNs}{TPs+TNs+FPs+FNs} \quad (7)$$

$$Sensitivity\ (Recall) = \frac{TPs}{TPs+FNs} \quad (8)$$

$$Precision = \frac{TPs}{TPs+FPs} \quad (9)$$

$$Specificity = \frac{TNs}{TNs+FPs} \quad (10)$$

$$\text{F-}score = \frac{2TPs}{2TPs+FPs+FNs} \quad (11)$$

This study assessed the efficacy of the proposed method on a test data set by measuring five parameters (Singh and Jaiswal, 2022), including accuracy, precision, sensitivity, specificity, and F-score, as defined in Equation 7-11. True positives (TPs) occurred when the actual value and the prediction were positive. In addition, True negatives (TNs) occurred when the actual value and prediction were negative. False positives (FPs) were when the actual outcome was negative while the forecast was positive. Following the discussion, FPs were also referred to as a type 1 error. False negatives (FNs), known as type 2 errors, occur when the actual result is positive, but the forecast is negative.

3. Results and Discussion

3.1. Dataset Evaluation

PERCLOS index value was obtained by Zheng and Lu (2017) using Equation 1. Figure 6 showed that this index of several subjects was distributed centrally without outliers, but there was also a large amount of unbalanced data. The class with the most significant sample showed tired conditions among the three classes. Only S16 tired index data was centered on the drowsy condition, and S20 was on the awake condition. Moreover, data sets S05, S14, S15, and S16 signified a slightly even distribution of samples, prompting these samples to be selected for further analysis.

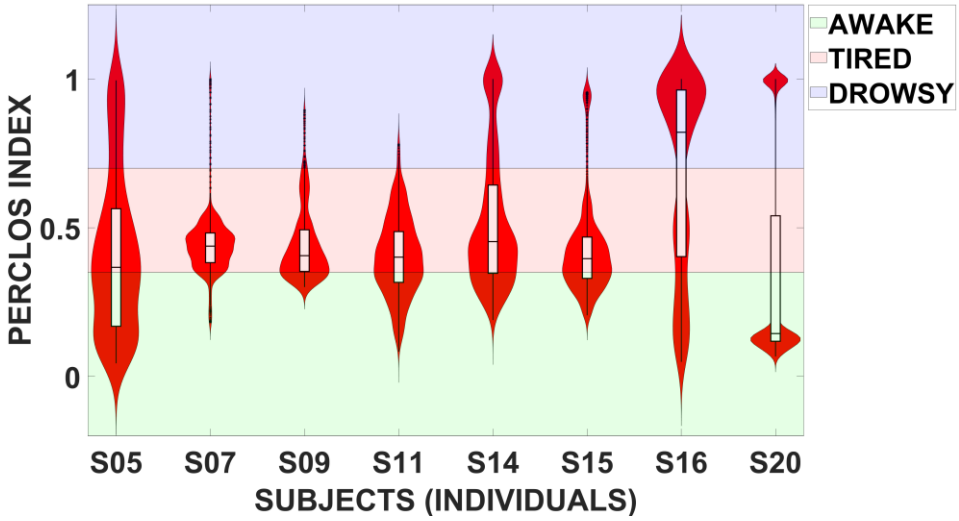

Figure 6 Distribution of PERCLOS index for each class in each subject

The efficiency of the classification model was affected by an imbalance in the number of samples. Models trained with imbalanced data showed bias towards the majority class because the models were optimized to reduce total error. Therefore, the model predicted predominantly the majority class, even though the cases were from the minority class. Unbalanced data led to a less-than-optimal performance for generalization, causing the model to face difficulty categorizing examples from the minority class. This model lacked sufficient examples to understand minority class characteristics effectively. Oversampling was a powerful method to overcome class imbalance in classification tasks, and it was used to affect class imbalance in a dataset by increasing the number of samples in minority classes to balance the class distribution. During the study, Equation 4 was used to balance the number of classes.

3.2. Scalp Topography Analysis

Scalp topography, also called brain mapping or scalp mapping, refers to the spatial distribution of neural activity across the scalp's surface as measured by EEG methods, as

shown in Figure 7. This mapping included the electric field generated by brain nerve activity to electrode locations on the scalp. Figure 7(a) showed a scalp topography using features from signal energy calculations using Equation 3, while 7(b) signified the signal energy filtered using Equation 2. From this graph, the spatial distribution and temporal dynamics of neural activity in the human brain when awake, tired, and drowsy were examined. The analysis offered a valuable understanding of the functional organization of the nervous system and its function in cognition processes, sensory perception, motor control, and clinical disorders for drivers. In addition, the graph showed significant differences in patterns for each subject and class. There was an increase in activity in the left temporal brain area in subjects S05 and S14 as the level of drowsiness increased. Different patterns of improvement were shown by subjects S15 and S16. Each subject and class signified various patterns, making concluding it generally challenging. The source of activity arose from different electrodes for each subject.

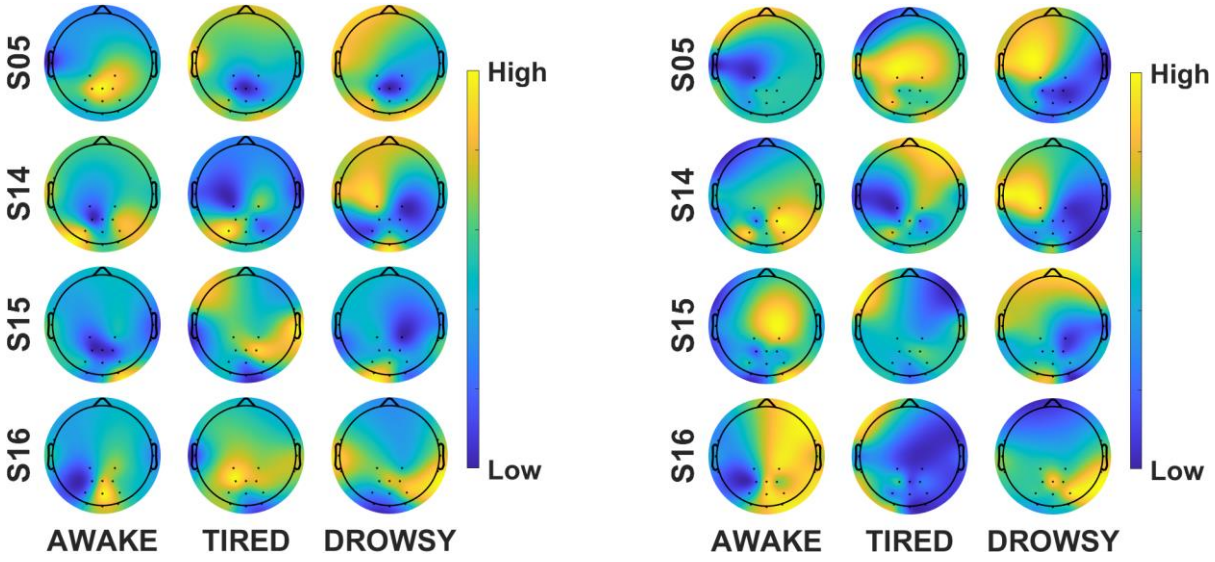

Figure 7 Scalp topographies using LSF (a) and Scalp topographies without using LSF (b).

The scalp topography produced by applying LSF varied from those without LSF. Topography without using LSF also showed different patterns for each subject and class. Moreover, the energy source was more localized than without using LSF. Visualization using LSF was more accurate because the energy from each electrode did not spread widely to match the electrode location. For example, in Figure 7(a), subject S15 in the class labeled drowsy acquired much energy in the frontal area where no electrodes were in the part. The outcome varied from the topography in Figure 7(b), which was in the exact location where the energy was more focused at electrode channel "O1". This result showed that LSF was more suitable for viewing energy sources that appeared in the topography.

3.3. Classification Performance of Each Subject

Classifying each subject, known as intra-subject classification, was a machine learning task aimed at classifying data samples in the same individual or subject. One method applied in this study was analyzing data from the same individual to produce predictions or diagnose conditions. Intra-subject classification analyzed data from each subject separately rather than combining data from multiple subjects. This method signified those subjects showed different patterns or characteristics in individual data, aiming for accurate classification or prediction. Four models were used in classification, and the results were compared to identify the model with the highest accuracy.

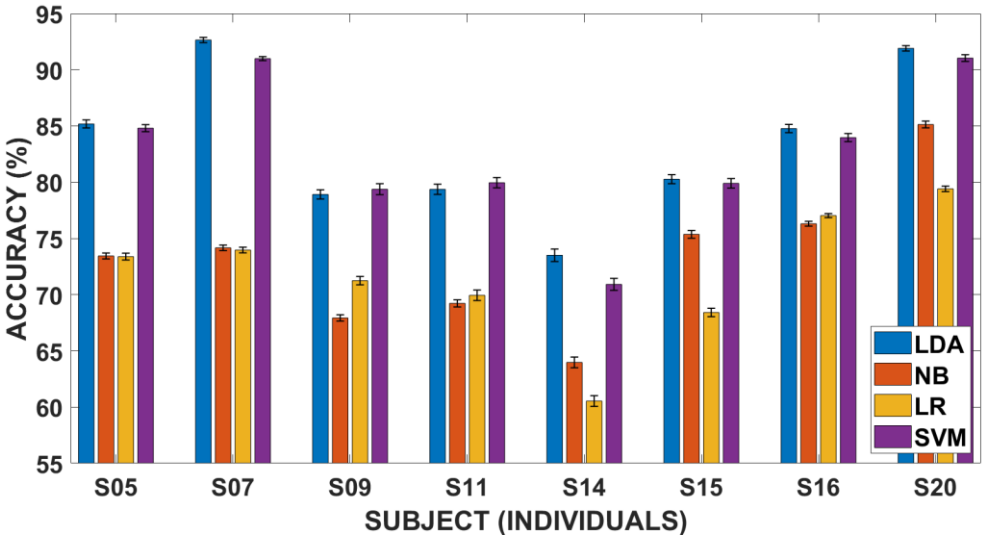

Figure 8 Classification accuracy without using LSF of each subject with different classifiers

During the study, all models showed accuracy values greater than 59%, and there was poor performance in NB and LR models, as shown in Figure 8 as well as 9. The outcome showed that the NB model had a higher average accuracy than the LR. The SVM model had the highest average accuracy of 84.27% in intra-subject classification. The accuracy of the LDA model produced an average accuracy nearly the same as SVM, which was 84.24%. The lowest accuracy of SVM occurred in subject S14, with an accuracy value of 70.50%, and the highest was in subject S07 at 93.05%. Moreover, a comparison of classification performance for each model with and without using LSF is shown in Figure 10. The comparison results showed that LSF did not improve classification performance with LDA and SVM models. However, LSF increased the average accuracy value in NB and LR classification models. Applying LSF also improved the standard deviation value, leading to less precise detection and a significant decrease in some classification results. Consequently, LSF was not recommended for vigilance detection-based EEG classification. Based on the comparison results in Figure 10, the SVM model was selected for cross-subject classification.

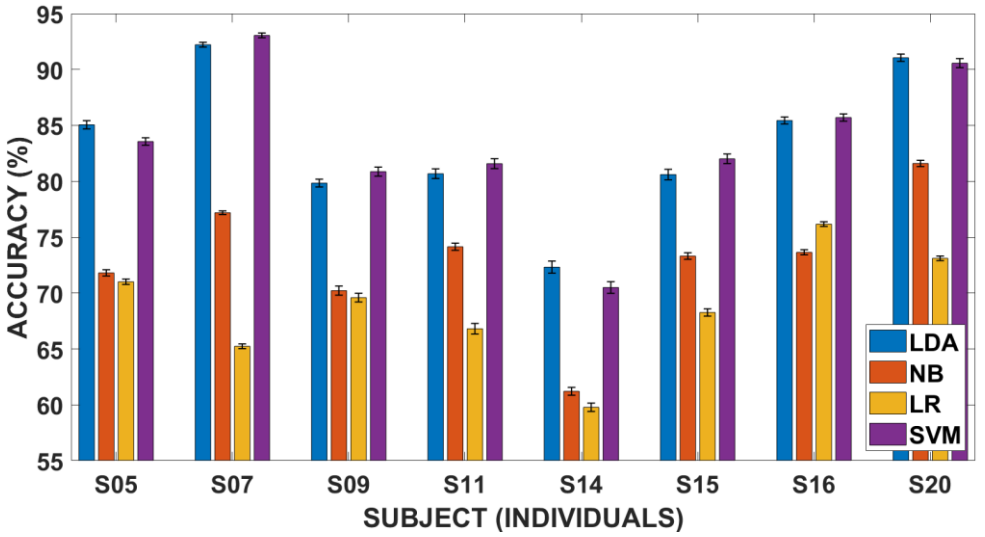

Figure 9 Classification accuracy using LSF of each subject with different classifiers

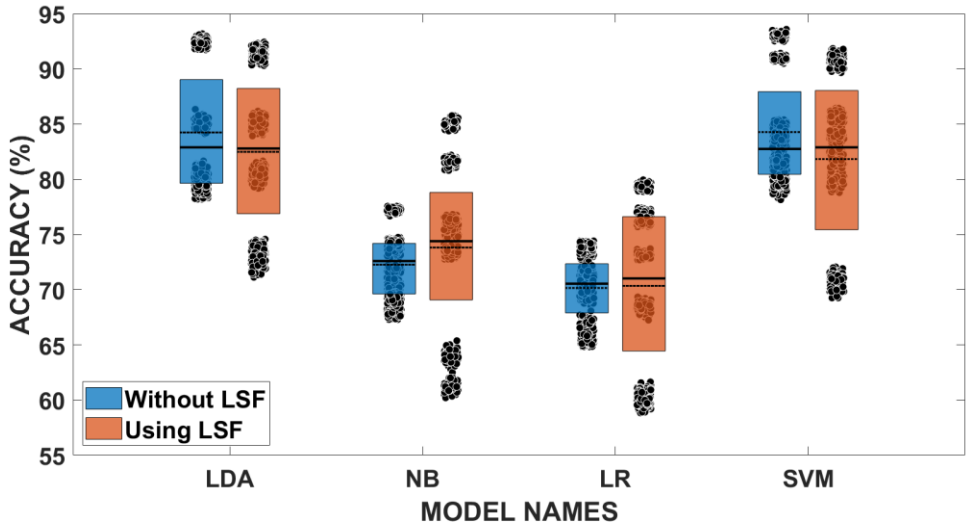

Figure 10 Comparison of the accuracy on each model with and without LSF

3.4. Result of Feature Selection

Feature selection in classification included performing selection by selecting a subset of pertinent features from the initial set to improve the model's performance or reduce computational complexity. This selection aimed to maintain the most informative and discriminative features when irrelevant, redundant, or distracting features are found. By selecting only the most relevant features, the dimensionality of the data was reduced, leading to simpler, easier-to-interpret models and faster computation. Additionally, the original features were kept when reducing features led to decreased accuracy. A comparative analysis of feature selection outcomes using KW and MRMR methods in Equations 5 and 6 is shown in Figure 11.

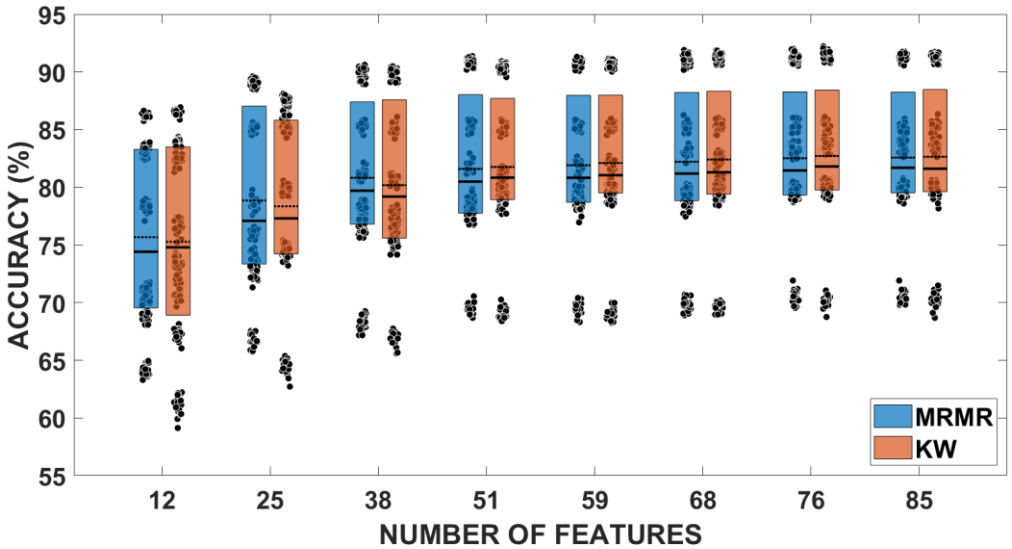

Figure 11 Comparison of accuracy on each number of features using the MRMR and KW algorithms

A total of eight groups were formed with a total of 85 features. Based on the computational results of KW and MRMR algorithms, the selection started from the lowest number, 12 to 85, with 15% and 10% intervals for each level. From the graph, a conclusion showed that reducing irrelevant features based on KW and MRMR significantly reduced accuracy. There was an increase in the minimum accuracy value when the quantity of

features had been elevated. The number of features with 68 was close to the maximum accuracy value. However, with 76 features, it had slightly higher accuracy and did not affect computer work significantly. During the study, 76 features were used for the classification process between subjects.

3.5. Classification Performance on Cross-Subject

Cross-subject classification aims to classify data samples from several individuals or subjects collectively. The method pooled data from all subjects, and the SVM model was randomly trained on the combined data set to predict or perform classification tasks. This classification also aimed to develop a strong classification model that generalized to different individuals or subjects by collecting data from multiple sources and capturing general patterns while accommodating individual variability. The confusion matrix was used to assess the effectiveness of the classification model, as shown in Figure 12(a). This matrix reviewed the predictions performed by the model compared to the actual labels or ground truth. The confusion matrix presented the aggregate count of events in each cell. Each row represented the specific classes, and the columns signified the projected classes. Moreover, the numbers in the diagonal boxes represented correctly classified observations, while the numbers in the boxes to the right showed misclassified observations. The terms "bottom" and "correspond" refer to how these classifications relate to the original observations.

The confusion matrix proved that the SVM model was strong in classifying drowsy classes, shown by the fewest errors when faced with other classes, namely categories with awake and tired labels. The model was misclassified 221 times among the total awake class of 722 data. In addition, SVM struggled to classify data with tired labels, leading to 352 prediction errors out of 1069 data. The model performance for each class was also supported by the receiver operating characteristic (ROC) curve, as shown in Figure 12(b). The characteristic curve showed the performance of the SVM model at all thresholds in different classifications. Additionally, the ROC graph signified that the y-axis represented the positive rate (also known as sensitivity), and the x-axis was the false positive rate (specificity subtracted from 1). Sensitivity refers to the proportion of positive events that were correctly classified. Moreover, the false positive rate represented the proportion of adverse events that were misclassified.

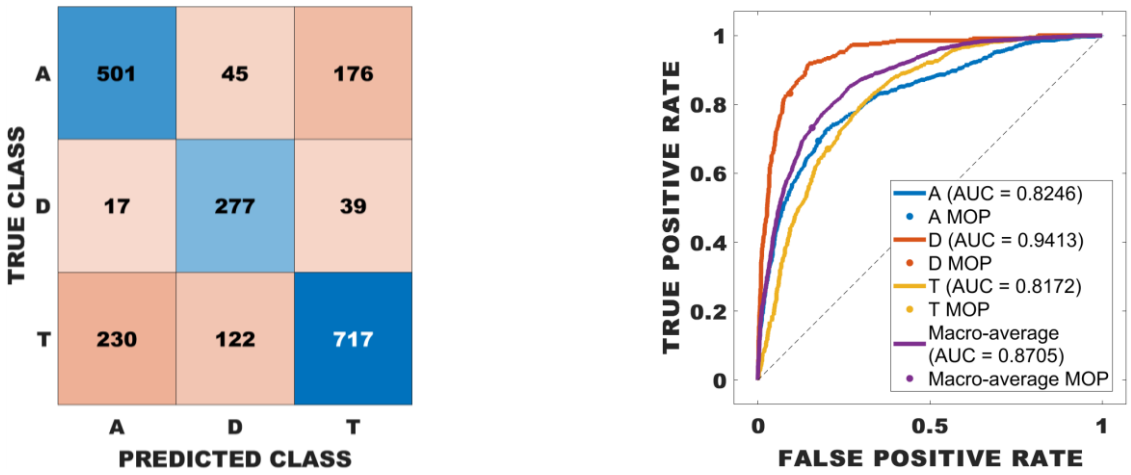

Figure 12 Confusion matrix (a) and ROC curve (b) of SVM performance on cross-subject classification.

The area under the ROC curve (AUC) measured the total performance of an SVM. AUC ranges from 0 to 1, where a rating of 1 signified flawless categorization and a value of 0.5

implied performance equivalent to random guessing. Following the discussion, higher AUC values showed better model performance, with values closer to 1 reflecting more substantial class discrimination. The graph signified that the class with the label drowsy had the most considerable AUC value, 94.13%. This result implied that the SVM model was the strongest in classifying data with the label drowsy rather than the labels awake and tired. The average AUC value for SVM classifying EEG based on driver tired was 87.05%.

Table 1 Cross-subject classification performance

Parameter	Class		
	Awake	Tired	Drowsy
True Positive	501	717	277
False Positive	247	215	167
False Negative	221	352	56
True Negative	1155	840	1624
Precision	0.6698	0.7693	0.6239
Sensitivity	0.6939	0.6707	0.8318
Specificity	0.8238	0.7962	0.9068
Accuracy	0.7039	0.7039	0.7039
F-Score	0.6816	0.7166	0.7130

During the study, Equation 7 was applied to the confusion matrix to calculate the model performance. The performance results of the SVM classification model in cross-subject classification as a whole are seen in Table 1. Additionally, the total accuracy value of the model was 70.39%, and the specificity parameter achieved the best values across all classes compared to other parameters. The specificity in this examination measured the ability to allocate a driver who was not drowsy, as two other class states, awake and tired, as the test had few FPs. Although the accuracy of inter-subject classification was lower compared to intra-subject, classifying between subjects in this study reflected real-world applications. Previous studies showed low accuracy in EEG classification cross-subject because of the dynamic nature of EEG over time and subject (Li *et al.,* 2023A; Liu *et al.,* 2023; Yuan *et al.,* 2023).

From the topographic maps in Figures 7(a) and 7(b), the finding showed that the application of LSF significantly influenced topographic patterns. This result signified that the energy was more focused on the electrode position when using LSF. Previous studies found that applying spatial filters to EEG data improved the performance of classification models (Tsuchimoto *et al.,* 2021; Alonso and Vellasco, 2016). Moreover, using LSF to drive vigilance-based EEG data only increased accuracy in a few subjects. The average accuracy value for classification using LSF did not increase compared to that without using LSF. In this case, LSF also led to lower precision values, shown by higher standard deviation values. The results proved that evaluating the implementation of LSF was essential since the effectiveness of applying LSF varied for each subject. Additionally, the differences in the distribution of EEG data for each subject were more significant compared to the subject of the topic.

4. Conclusions

In conclusion, LSF was applied to each brain signal frequency band using an equation that calculated the energy possessed by each channel and band. During this study, a BCI vigilance investigation was conducted to examine brain activity patterns of vigilance states in a driving task, and four classification models were compared. The signal visualization method was adopted to explore and compare patterns of vigilance estimates across subjects in a driving task. Moreover, topographic patterns using the LSF algorithm signified

substantial differences. The results of using LSF showed the energy that appeared was related to the location of the electrode. LSF increased variability in all classification models, and accuracy decreased significantly in SVM and LDA. Following the process, the results of applying KW and MRMR-type feature selection algorithms showed the best reduction in the number of features by 76 of the total number of features. KW algorithm had better feature quality with a higher average value and minimum accuracy with the same number of features. In this study, four types of classification models were used, namely LDA, LR, NB, and SVM. The classification results specified that using the signal energy features without LSF and SVM model was the most accurate when applied to intra-subject and cross-subject classification schemes. The intra-subject accuracy value was 84.27%, and across the subject was 70.39%.

Symbols

e	Electrode voltage	N	Total observation count across all groups
$e^{Laplace}$	Laplacian spatial filter	r	A random number between 0 and 1
E_s	Signal energy	R	Ranks of the observations in a group
f	Candidate feature	S	Set of selected features
H	Kruskal – Wallis	x'	SMOTE
I	Mutual information	x	Original sample
K	Number of neighboring electrodes	Y	Target variable
k	Number of clusters	z	The closest sample

Abbreviations

ANOVA	Analysis of variance	MOP	Model Operating Point
AUC	Area under the curve	MRMR	Maximum relevance - minimum redundancy
AV	Automated vehicle	NB	Naïve Bayes
BCI	Brain-computer interface	O	Occipital
CP	Central – parietal	OZ	Occipital – zero
EEG	Electroencephalogram	P	Parietal
EOG	Electrooculogram	PERCLOS	Percentage of eye closure
FIR	Finite impulse response	PO	Parietal – occipital
FNs	False negative	POZ	Parietal – occipital - zero
FPs	False positive	PZ	Parietal – zero
FT	Frontal – temporal	ROC	Receiver operating characteristic
IC	Independent component	SAE	Society of Automotive Engineers
ICA	Independent Component Analysis	SMOTE	Synthetic minority oversampling technique
KW	Kruskal – Wallis	SVM	Support vector machine
LCD	Liquid crystal display	T	Temporal
LDA	Linear discriminant analysis	TNs	True negative
LR	Logistic regression	TP	Temporal - parietal
LSF	Laplacian spatial filter	TPs	True positives

Acknowledgment

The authors are grateful to Mercu Buana University for the financial assistance under contract No. 02-5/725/B-SPK/III/2024 and the Beijing Institute of Technology.

References

Alonso, D.R., Vellasco, M.M.B.R., 2016. Spatial Filter Comparison for a Brain Computer Interface. *In:* 2016 IEEE Latin American Conference on Computational Intelligence (LA-CCI), pp. 1–6, doi: 10.1109/LA-CCI.2016.7885718

Arefnezhad, S., Samiee, S., Eichberger, A., Nahvi, A., 2019. Driver Drowsiness Detection Based on Steering Wheel Data Applying Adaptive Neuro-Fuzzy Feature Selection. Sensors, Volume 19(4), p. 943, doi: 10.3390/S19040943

Bi, L., Xia, S., Fei, W., 2021. Hierarchical Decoding Model of Upper Limb Movement Intention from EEG Signals Based on Attention State Estimation. *Institute of Electrical and Electronics Engineers (IEEE) Transactions on Neural Systems and Rehabilitation*, Volume 29 pp. 2008–2016, doi: 10.1109/TNSRE.2021.3115490

Cui, M., Wang, C., Lv, Y., Yu, W., Guo, H., Tian, Y., 2022. Human-Like Behavior Decision Making Method for Intelligent Vehicle Considering Driver Characteristics. *In:* 2022 6th CAA International Conference on Vehicular Control and Intelligence (CVCI), pp. 1–6, doi: 10.1109/CVCI56766.2022.9964503

Di, Y., An, X., He, F., Liu, S., Ke, Y., Ming, D., 2019. Robustness Analysis of Identification using Resting-State Electroencephalogram (EEG) Signals. *Institute of Electrical and Electronics Engineers (IEEE) Access*, Volume 7, pp. 42113–42122, doi: 10.1109/ACCESS.2019.2907644

Gan, J., Li, S., Wei, C., Deng, L., Tang, X., 2023. Intelligent Learning Algorithm and Intelligent Transportation-Based Energy Management Strategies for Hybrid Electric Vehicles: A Review. *Institute of Electrical and Electronics Engineers (IEEE) Transactions on Intelligent Transportation Systems*, Volume 24(10), pp. 10345–10361, doi: 10.1109/TITS.2023.3283010

Gaur, P., Chowdhury, A., McCreadie, K., Pachori, R.B., Wang, H., 2021. Logistic Regression with Tangent Space Based Cross-Subject Learning for Enhancing Motor Imagery Classification. *Institute of Electrical and Electronics Engineers (IEEE) Transactions on Cognitive and Developmental Systems*, Volume 14(3), pp. 1188–1197, doi: 10.1109/TCDS.2021.3099988

Gupta, A., Vardhan, H., Singh, S., Khandelwal, S., 2023. Vigilance Monitoring for Safer Driving and Passenger Protection using ML. *In:* 2023 8th International Conference on Communication and Electronics Systems (ICCES), pp. 1191–1197, doi: 10.1109/ICCES57224.2023.10192874

Lazcano-Herrera, A.G., Fuentes-Aguilar, R.Q., Ramirez-Morales, A., Alfaro-Ponce, M., 2023. BiLSTM and SqueezeNet with Transfer Learning for EEG Motor Imagery Classification: Validation with Own Dataset. *Institute of Electrical and Electronics Engineers (IEEE)* Access, Volume 11, pp. 136422–136436, doi: 10.1109/ACCESS.2023.3328254

Li, G., Zhang, L., Zou, Y., Ouyang, D., Yuan, Y., Lian, Q., Chu, W., Guo, G., 2023A. Driver Vigilance Detection Based on Limited Electroencephalography (EEG) Signals. *Institute of Electrical and Electronics Engineers (IEEE)* Sensors Journal, Volume 23(12), pp. 13387–13398, doi: 10.1109/JSEN.2023.3273556

Li, W., Cui, Y., Ma, Y., Chen, X., Li, G., Zeng, G., Guo, G., Cao, D., 2023B. A Spontaneous Driver Emotion Facial Expression (DEFE) Dataset for Intelligent Vehicles: Emotions Triggered by Video-Audio Clips in Driving Scenarios. *Institute of Electrical and Electronics*

Engineers (IEEE) Transactions on Affective Computing, Volume 14(1), pp. 747–760, doi: 10.1109/TAFFC.2021.3063387

Li, W., Tan, R., Xing, Y., Li, G., Li, S., Zeng, G., Wang, P., Zhang, B., Su, X., Pi, D., Guo, G, Cao, D., 2022b. A Multimodal Psychological, Physiological and Behavioural Dataset for Human Emotions in Driving Tasks. *Scientific Data*, Volume 9(1), pp. 1–20, doi: 10.1038/s41597-022-01557-2

Li, Z., Chen, L., Nie, L., Yang, S.X., 2022a. A Novel Learning Model of Driver Fatigue Features Representation for Steering Wheel Angle. *Institute of Electrical and Electronics Engineers (IEEE)* Transactions on Vehicular Technology, Volume 71(1), pp. 269–281, doi: 10.1109/TVT.2021.3130152

Li, Z., Li, S.E., Li, R., Cheng, B., Shi, J., 2017. Driver Fatigue Detection using Approximate Entropic of Steering Wheel Angle from Real Driving Data*. International Journal of Robotics and Automation*, Volume 32(3), pp. 291–298, doi: 10.2316/JOURNAL.206.2017.3.206-4972

Liu, S., Wang, Z., An, Y., Li, B., Wang, X., Zhang, Y., 2023. DA-Capsnet: A Multi-Branch Capsule Network Based on Adversarial Domain Adaption for Cross-Subject Electroencephalogram (EEG) Emotion Recognition. *Knowledge-Based Systems*, Volume 283, p. 111137, doi: 10.1016/J.KNOSYS.2023.111137

Luna, F.G., Tortajada, M., Martín-Arévalo, E., Botta, F., Lupiáñez, J., 2022. A Vigilance Decrement Comes Along with an Executive Control Decrement: Testing the Resource-Control Theory. *Psychonomic Bulletin and Review*, Volume 29(5), pp. 1831–1843, doi: 10.3758/S13423-022-02089-X/FIGURES/4

Maimaiti, P., Sen, L.F., Aisilahong, G., Maimaiti, R., Yun, W.Y., 2020. Retraction Notice to 'Statistical Analysis with Kruskal Wallis Test for Patients with Joint Contracture' [Future Gener. Comput. Syst. 92 (2019) 419–423]. *Future Generation Computer Systems, North-Holland*, Volume 107, p. 1153, doi: 10.1016/J.FUTURE.2020.02.064

Nacpil, E.J.C., Wang, Z., Guan, M., Nakano, K., Jeon, I., 2023. EEG-Based Emergency Braking Prediction using Data Ablation and SVM Classification. *Institute of Electrical and Electronics Engineers (IEEE) Sensors Journal.* Volume 23(14), pp. 16013–16019, doi: 10.1109/JSEN.2023.3283447

Nurfirdausi, A.F., Apsari, R.A., Wijaya, S.K., Prajitno, P., Ibrahim, N., 2022. Wavelet Decomposition and Feedforward Neural Network for Classification of Acute Ischemic Stroke Based on Electroencephalography. *International Journal of Technology*, Volume 13(8), pp. 1745–1754, doi: 10.14716/IJTECH.V13I8.6132

Othmani, A., Sabri, A.Q.M., Aslan, S., Chaieb, F., Rameh, H., Alfred, R., Cohen, D., 2023. EEG-Based Neural Networks Approaches for Fatigue and Drowsiness Detection: A Survey*. Neurocomputing,* Volume 557, p. 126709, doi: 10.1016/J.NEUCOM.2023.126709

Oztel, G.Y., 2021. Vision-Based Road Segmentation for Intelligent Vehicles using Deep Convolutional Neural Networks. *In:* 2021 International Conference on Innovations in Intelligent Systems and Applications, INISTA 2021, p. 1–5, doi: 10.1109/INISTA52262.2021.9548601

Pion-Tonachini, L., Kreutz-Delgado, K., Makeig, S., 2019. ICLabel: An Automated Electroencephalographic Independent Component Classifier, Dataset, and Website. *NeuroImage*, Volume 198, p. 181, doi: 10.1016/J.NEUROIMAGE.2019.05.026

Pranoto, H., Wahab, A., Adriansyah, A., Feriyanto, D., 2023. Internet of Thing Development for Fatigue Analyzer Device Control for Truck and Bus Engine. *In:* Proceedings, American Institute of Physics Inc (AIP) Conference Proceedings, Volume 2671(1), doi: 10.1063/5.0116314/2880385

Rogel, J.M.H., Martínez Beltrán, E.T., Quiles Pérez, M., López Bernal, S., Martínez Pérez, G. and Huertas Celdrán, A. (2024), "Studying drowsiness detection performance while driving through scalable machine learning models using electroencephalography", Cognitive Computation, Springer, Vol. 16 No. 3, pp. 1253–1267, doi: 10.1007/S12559-023-10233-5/TABLES/12, doi: 10.1007/S12559-023-10233-5/TABLES/12

Sharmila, A., Geethanjali, P., 2016. DWT Based Detection of Epileptic Seizure from EEG Signals Using Naive Bayes and K-NN Classifiers. *Institute of Electrical and Electronics Engineers (IEEE) Access*. Volume 4, pp. 7716–7727, doi: 10.1109/ACCESS.2016.2585661

Singh, B., Jaiswal, R., 2022. A Study on Classifiers for Temporal Data. *In:* Proceedings - 2022 IEEE 11th International Conference on Communication Systems and Network Technologies (CSNT) 2022. pp. 305–313, doi: 10.1109/CSNT54456.2022.9787640

Siuly, S., Khare, S.K., Bajaj, V., Wang, H., Zhang, Y., 2020. A computerized method for automatic detection of schizophrenia using EEG signals. *Institute of Electrical and Electronics Engineers (IEEE) Transactions on Neural Systems and Rehabilitation Engineering*, Volume 28(11), pp. 2390–2400, doi: 10.1109/TNSRE.2020.3022715

Song, C., Zhao, T., Xu, L., Huang, X., 2024. Probabilistic Prediction of Uniaxial Compressive Strength for Rocks from Sparse Data using Bayesian Gaussian Process Regression with Synthetic Minority Oversampling Technique (SMOTE), *Computers and Geotechnics*, Volume 165, p. 105850, doi: 10.1016/J.COMPGEO.2023.105850

Teng, T., Bi, L., Liu, Y., 2018. EEG-Based Detection of Driver Emergency Braking Intention for Brain-Controlled Vehicles. *Institute of Electrical and Electronics Engineers (IEEE) Transactions on Intelligent Transportation Systems*. Volume 19(6), pp. 1766–1773, doi: 10.1109/TITS.2017.2740427

Tsuchimoto, S., Shibusawa, S., Iwama, S., Hayashi, M., Okuyama, K., Mizuguchi, N., Kato, K., Ushiba, J., 2021. Use of Common Average Reference and Large-Laplacian Spatial-Filters Enhances EEG Signal-To-Noise Ratios in Intrinsic Sensorimotor Activity. *Journal of Neuroscience Methods*, Volume 353, doi: 10.1016/J.JNEUMETH.2021.109089

Wang, Y., Fang, Z., Sun, X., Lin, X., Niu, L., Ma, W., 2023. An Adaptive Driver Fatigue Classification Framework Using EEG and Attention-Based Hybrid Neural Network with Individual Feature Subsets. Biomedical Signal Processing and Control, Volume 85, p. 105045, doi: 10.1016/J.BSPC.2023.105045

Yu, H., Lu, H., Wang, S., Xia, K., Jiang, Y., Qian, P., 2019. A General Common Spatial Patterns for EEG Analysis with Applications to Vigilance Detection. *Institute of Electrical and Electronics Engineers (IEEE)* Access. Volume 7, pp. 111102–111114, doi: 10.1109/ACCESS.2019.2934519

Yuan, D., Yue, J., Xiong, X., Jiang, Y., Zan, P., Li, C., 2023. A Regression Method for EEG-Based Cross-Dataset Fatigue Detection. *Frontiers in Physiology*, Frontiers Media SA, Volume 14, doi: 10.3389/fphys.2023.1196919

Yue, M., Geng, X., Wang, L., Zhang, X., 2022. An Artifact Removing Method Fusing Fastica and CNN for EEG Signal. *In:* Proceedings - 2022 International Conference on Intelligent Transportation, Big Data and Smart City (ICITBS) 2022, pp. 22–25, doi: 10.1109/ICITBS55627.2022.00014

Zainy, M.L.S., Pratama, G.B., Kurnianto, R.R., Iridiastadi, H., 2023. Fatigue Among Indonesian Commercial Vehicle Drivers: A Study Examining Changes in Subjective Responses and Ocular Indicators. *International Journal of Technology*, Volume 14(5), pp. 1039–1048, doi: 10.14716/IJTECH.V14I5.4856

Zhang, C., Eskandarian, A., 2021. A Survey and Tutorial of EEG-Based Brain Monitoring for Driver State Analysis. *Institute of Electrical and Electronics Engineers (IEEE) /CAA*

Journal of Automatica Sinica, Volume 8(7), pp. 1222–1242, doi: 10.1109/JAS.2020.1003450

Zhang, G., Etemad, A., 2021. Capsule Attention for Multimodal EEG-EOG Representation Learning with Application to Driver Vigilance Estimation. *Institute of Electrical and Electronics Engineers (IEEE) Transactions on Neural Systems and Rehabilitation Engineering*. Volume 29, pp. 1138–1149, doi: 10.1109/TNSRE.2021.3089594

Zheng, W.L., Lu, B.L., 2017. A Multimodal Approach to Estimating Vigilance Using EEG and Forehead EOG. *Journal of Neural Engineering.* Volume 14(2), doi: 10.1088/1741-2552/aa5a98

Zhou, S., 2023. Research On Automatic Driving Vehicle Auxiliary System Based on Computer Intelligent Network. *In:* 2023 Estimation. *Institute of Electrical and Electronics Engineers (IEEE)* 3rd International Conference on Power, Electronics and Computer Applications (ICPECA) 2023. pp. 1573–1578, doi: 10.1109/ICPECA56706.2023.10075905

Zuraida, R., Wijayanto, T., Iridiastadi, H., 2022. Fatigue During Prolonged Simulated Driving: an Electroencephalogram Study*. International Journal of Technology*, Volume 13(2), pp. 286–296, doi: 10.14716/IJTECH.V13I2.4820